# Bacterial species and surface structures shape gene transfer and the transcriptional landscape during early conjugation

Galain C Williams[1], Jillian C Danne[2], Simon Crawford[2], Jihane Homman-Ludiye[3], Xenia Kostoulias[4], Bailey Heron[1], Tasnia Islam[1], Melvin Yong[5], Yunn-Hwen Gan[5], Yogitha N Srikhanta[1,6] and Dena Lyras[1,6†]

[1]Infection Program, Monash Biomedicine Discovery Institute and Department of Microbiology, Monash University, Clayton, Victoria Australia, 3800.

[2]Monash Ramaciotti Centre for Cryo-Electron Microscopy, A Node of Microscopy Australia, Monash University, Clayton, Victoria, Australia, 3800.

[3]Monash Micro Imaging, Monash University, Clayton, Victoria, Australia, 3800.

[4]Department of Infectious Diseases, The Alfred Hospital and School of Translational Medicine, Monash University, VIC, Australia, 3004

[5]Infectious Diseases Translational Research Program, Department of Biochemistry, Yong Loo Lin School of Medicine, National University of Singapore, Singapore, Singapore, 117596.

[6]Joint senior author; these authors contributed equally to this article

Corresponding Author: Professor Dena Lyras

**Email:** Dena.Lyras@monash.edu

**Author Contributions:** G.W. co-designed experiments, performed the majority of the experimental work and co-wrote the manuscript. J.D. and S.C. performed the TEM and assisted with SEM imaging. J.H. assisted with fluorescent microscopy imaging and analysis. X.K. assisted with RNA sequencing. B. H. assisted with fluorescent microscopy. T. I. assisted with conjugation time course experiments. M.Y. and Y.H.G assisted with the *K. pneumoniae* conjugation experiments and experimental design. Y.N.S. co-wrote manuscript & co-designed the majority of experiments. D.L. co-designed all experiments and co-wrote the manuscript.

**Competing Interest Statement:** No Competing Interests

**Keywords:** Bacterial Conjugation; Plasmid Transfer; Antibiotic Resistance; Broad host range plasmids; mobile genetic elements

**Abstract**

Conjugative plasmids drive bacterial evolution and niche adaptation. Their carriage often corresponds with changes to the host transcriptome, but it is unknown during which stage of the conjugation process these transcriptional changes are initiated, and how gene transfer is modulated as they occur. This is because they are normally studied after their full acquisition by conjugation has already occurred, not during the process. Here, active RP4 conjugation revealed that the transcriptional response to plasmid acquisition is almost immediate and is host and surface factor dependent. Responses included activation of non-SOS stress pathways, motility, exopolysaccharide production, anaerobic respiration, and metabolic adaptation. These responses were not a barrier to conjugation, indicating that their significance relates to host homeostasis rather than gene transfer. The recipient could prevent these responses by blocking conjugation through capsule expression. RP4 expression was also inhibited by recipient capsule, since capsule physically blocked donor-recipient contact. Unexpectedly, within a population, RP4 was found to exploit single cell variation in recipient capsule thickness and to successfully conjugate with recipient bacteria with reduced capsule. These results show a novel interplay between plasmid and surface architecture across diverse species that controls the conjugation transcriptional landscape, with important ramifications for plasmid dissemination and evolution.

## Main Text

## Introduction

Plasmid dissemination by bacterial conjugation contributes to rapid change in bacteria, exemplified by the continuing emergence of highly virulent antibiotic resistant bacterial pathogens (1). During conjugation plasmid DNA is translocated into an apparently passive recipient cell from an active donor cell via a type 4 secretion system (T4SS) (2). Plasmid carriage can have a profound impact on the transcriptional profile of both host and plasmid (3), bacteria isolated following plasmid acquisition often exhibit altered expression of metabolic, respiration, transport, virulence, and other pathways (4-7). Apart from the SOS response which is induced by ssDNA entry into the recipient (8), it is unclear what broader

59 transcriptional changes occur within the recipient during the active conjugation process as
60 plasmid-host responses are typically studied 20-40 generations after the plasmid was
61 acquired. Similarly, whether these responses act as barriers or facilitators of conjugation
62 remains unknown.

63 Indeed, while no recipient factors have yet been identified as truly essential for conjugation
64 (9, 10), recent studies have highlighted an increasingly important role for the recipient in
65 conjugation. The composition of the recipient plasma membrane can impact conjugation
66 frequencies (11), as can the presence of capsules (12) and cognate accessory receptors
67 (13). Recipient bacteria respond to conjugation through the expression of SOS pathways,
68 and consequently plasmids have evolved suppressors of the recipient SOS response (14,
69 15). These suppressors are likely to protect recipient bacteria from deleterious SOS-
70 enhanced recombination (16). Although a picture of an indirect role for the recipient during
71 the conjugation process is beginning to emerge, a deeper understanding of how recipient
72 bacteria respond to, and govern, foreign DNA acquisition is needed because this process
73 directly facilitates the evolution of traits problematic for human, animal and environmental
74 health.

75 In this study, we examined how recipient bacteria respond to and modulate the active
76 conjugation of plasmid RP4 using a transcriptomic and imaging-based approach.
77 Transcriptional analysis of a recipient that was proficient for RP4 conjugation (conjugation-
78 permissive), *E. coli*, revealed that conjugation greatly alters the recipient transcriptional
79 profile almost immediately upon exposure to the donor. This response included the
80 expression of mixed stress adaptations, anerobic respiratory pathways, motility, colanic
81 acid production, and metabolic pathways. However, this pronounced response did not
82 seem to ultimately impact RP4 acquisition, suggesting it is either not a barrier to
83 conjugation or that RP4 encodes mechanisms to overcome it. We also observed that RP4
84 gene expression was globally activated during *E. coli* conjugation, which resembled past
85 transcriptional studies of RP4 during *E. coli* conjugation (17).

86 When we repeated these experiments with *K. pneumoniae,* a poor recipient due to its
87 capsule (non-conjugation-permissive), we observed only a small transcriptional response,
88 and no activation of RP4 genes within the donor. Conversion of *K. pneumoniae* to a state

89 that was proficient for conjugation (conjugation-permissive) by capsule deletion restored
90 RP4 conjugation, leading to a greater recipient response that whilst mostly unique to *K.*
91 *pneumoniae*, did involve genes shared with *E. coli* that are known to impact conjugation
92 when deleted in the recipient. RP4 gene expression was also activated by the presence
93 of unencapsulated *K. pneumoniae*, with DNA mobilisation genes in particular increased in
94 expression. We resolved the mechanism through which capsule inhibits conjugation using
95 electron and fluorescence microscopy. This analysis revealed that capsule is a physical
96 barrier to donor-recipient outer membrane contact, preventing mating pair formation and
97 RP4 gene activation in the donor. Unexpectedly, we discovered that single cell variation
98 in capsule thickness within *K. pneumoniae* populations gave rise to the small number of
99 transconjugants typically observed in RP4 conjugations with capsulated *K. pneumoniae*.
100 Our findings highlight that recipient species, and their surface structures directly shape
101 both conjugation, and the transcriptional landscape of the recipient and plasmid during
102 actively occurring conjugation.

## 103 Results

104

### 105 RP4 conjugation elicits the rapid activation of non-SOS stress, respiratory and 106 metabolic adaptation pathways in a conjugation-permissive recipient

107

108 To assess recipient and plasmid transcriptional activity with a conjugation-permissive
109 recipient, RNA-seq was performed on actively conjugating donor *E. coli* LT101(pVS520)
110 (phylogroup A), carrying an RP4 derivative pVS520, and the genetically distant recipient
111 *E. coli* DLL7555 (phylogroup B2). Based on a conjugation time course, we extracted RNA
112 15 minutes after donor-recipient mixing, when 15% of the recipient population had
113 received RP4, but conjugation was still actively occurring (Fig 1a). RNA was also extracted
114 from mock-conjugations between the same strains without pVS520, and from the donor
115 LT101(pVS520) alone without a recipient.

116 To determine how recipient *E. coli* DLL7555 responded to RP4 conjugation, we compared
117 gene expression of DLL7555 between the conjugation and mock conjugation conditions.
118 The many nucleotide differences between DLL7555 and LT101 (>78,000 genetic
119 variations within core genome) enabled effective recovery of strain-specific reads by

120 alignment against a concatenated LT101-DLL7555 reference sequence in which reads
121 aligning to both strains were discarded. We identified 130 differentially expressed genes,
122 88 upregulated and 42 downregulated (Fig 1b). These involved genes associated with
123 adaption and aversion to external stressors, which we have termed a mixed-stress
124 response, including temperature shock (*cspG*, *hslJ, deaD*), pH regulation (*yagU, ygaC,*
125 *ybay, speF*), osmotic shock (*osmB, osmY, nhaA*) and others (*mliC, soxS, rcsA, phoR*).
126 This response was paired with increased expression of colanic acid production (*wzc, wzb,*
127 *cpsB, wcaJ, wcaI, wcaE, wcaC, wcaA, gmd, fcl, wza, wcaD*), exopolyscharide production
128 (*yjbG, yjbF, yjbH*), and flagella production (*fliN, fliM, flgG, flgF, glgI, flgH, flhA, fliO*) genes,
129 responses associated with aversion to stressors and biofilm formation. Curiously, despite
130 an increase in flagella expression, the master flagella transcriptional regulator *flhD* was
131 decreased in expression, whilst the flagella anti-sigma factor *flgM* was increased. As some
132 conjugative plasmids induce biofilm formation following acquisition, we predicted that the
133 genes identified were involved with the induction of a recipient biofilm in the conjugation
134 mixture. Unexpectedly, however, we determined that DLL7555 co-culture with
135 LT101(pVS520) had a slight reduction in biofilm formation compared to the LT101 co-
136 culture, or monoculture (Supplementary Fig 1). This minor reduction may result from the
137 decreased expression of key biofilm formation factors encoded by *csgD* and *csgG* during
138 conjugation.

139 Unexpectedly, conjugation was also associated with increased expression of anaerobic
140 respiration and energy generation pathways (*fdnI, dmsB, napC, narG, narH, narI, hycF,*
141 *nrfA, nrfD, nrfC, nirB, fumB, dcuC*) which overlapped with inorganic nutrient metabolism
142 and nitrogen cycle metabolic processes (*napG, napH, narG, narH, narI, nrfA, narJ, nirB,*
143 *nirD, narK, napC*). Curiously, multiple siderophore, iron transport and iron homeostasis
144 pathways were downregulated, including (*fiu, cirA, fepA, fyuA, efeO, efeU, efeB, fhuE,*
145 *entD, entC, entF, chuA, chuS, chuT)*, though the master iron uptake regulator *fur* was not
146 differentially expressed.

147 GO term analysis reflected the multi-factorial recipient response to RP4 conjugation with
148 terms associated with stressors, respiratory pathways, and metabolic adaption being
149 significant (Fig 1c). Collectively, our findings suggest that early conjugation is both highly

150 stressful, and energetically intensive, for the recipient, requiring the activation of
151 respiratory pathways not typically present during aerobic growth whilst modulating iron
152 acquisition and homeostasis for an unknown reason. Our findings may explain the prior
153 observation that nascent RP4 transconjugants are growth impaired (18).

154 Finally, although our experiment was not designed to resolve donor-recipient specific
155 differences in RP4 expression, by comparison against the donor alone we reasoned we
156 could gain insight into the global expression pattern of RP4 across the entire conjugating
157 population. This comparison revealed increased expression of 47 pVS520-encoded genes
158 associated with DNA mobilisation (MOB), mating pair formation (MPF), Regulation and
159 replication, host-kill functions (*kil*), and other processes, a response entirely consistent
160 with previous reports of RP4 gene expression during *E. coli* conjugation (17) (Fig 1d).

161 **The recipient conjugation response is diminished by capsule but expressed in its**
162 **absence.**

163 To determine how a non-conjugation-permissive recipient reacts to an RP4 donor and
164 whether making it conjugation-permissive would produce an *E. coli*-like recipient
165 response, we examined conjugation in strains producing or not producing a capsule.
166 Capsule was used as the basis for non-permissiveness because it strongly blocks
167 conjugation but its removal through genetic deletion allows conjugation to proceed with
168 high efficiency (19). Capsule was also chosen because it differs from other mechanisms
169 like restriction-modification systems, which do not prevent conjugation, but instead prevent
170 plasmid establishment.

171 To identify a suitable capsulated recipient, we compared conjugation frequencies between
172 *Klebsiella pneumoniae* B5055, *Acinetobacter baumannii* AB5075, and *Pasteurella*
173 *multocida* VP161, against their respective acapsular derivatives (Supplementary Fig 2).
174 Whilst capsule hindered conjugation in all three species, only the acapsular *K.*
175 *pneumoniae* B5055Δ*wzbc* achieved conjugation frequencies comparable to *E. coli*
176 DLL7555. As a high frequency is essential for effectively resolving the recipient's
177 transcriptional response, we therefore performed RNA-seq on conjugation mixtures using

178 donor LT101(pVS520) with *K. pneumoniae* B5055 or B5055Δ*wzbc* recipients as before
179 with *E. coli* DLL7555.

180 The non-conjugation-permissive B5055 response to donor co-culture involved 10
181 differentially expressed genes (*carB, carA, lysS, clbS, glnH,* 08025*, glnP,* 08030, 08050,
182 08045*)*, with mostly decreased expression (Fig 2a). GO-term analysis identified terms
183 associated with sucrose catabolism, L-arginine biosynthesis and nucleotide biosynthesis
184 (Fig 2b). Conversion of B5055 to a conjugation-permissive state greatly bolstered the
185 response, with 54 B5055Δ*wzbc* genes being differentially expressed (Fig 2a). We
186 observed Increased expression of mixed stress adaptations that were seen in *E. coli* (*cspD*
187 and *nhaA*), but also those unique to B5055Δ*wzbc* (*loiP*, *ychH, hcp*). We also observed
188 increased expression of genes for carbohydrate transport (*araH, fucP, galP, manY, manZ,*
189 *manX, bglF*) and catabolism (*treC, fruK pck, bglB, opbG*). Broader transmembrane
190 transport genes (*psuT, sdaC, ompC, ttdT, nhaA, yebQ, malE, gntT, ompW*) were also
191 differentially expressed, which together suggest that increased substrate efflux across the
192 cell envelope may occur in B5055Δ*wzbc* during conjugation, along with altered
193 carbohydrate metabolism. Some of these genes were associated with growth under
194 anaerobic conditions (*ompW*, *ttdT*) alongside anaerobic respiration genes (*fdnG, fdhF,*
195 *narG*). GO-term analysis also identified terms for mixed stress responses and for altered
196 carbohydrate transport and metabolism (Fig 2b).

197 To determine how many genes were common between DLL7555 and B5055Δ*wzbc*, blast
198 was used to identify homologues within respective gene lists (Fig 2c). This revealed that
199 13 differentially expressed genes were shared between DLL7555 and B5055Δ*wzbc,*
200 indicating that approximately 10% of the permissive-recipient response is shared. These
201 included *ysab, galP, ypfG, ypeC, ompW, narG, cspG, citT, nhaA,* ACPEGL_23855*, ytjA*
202 with increased expression and *csgD* and *ompF* with decreased expression. Notably,
203 previous studies have shown that *nhaA* and *ompW* reduce conjugation when disrupted in
204 recipient bacteria (10, 13). Finally, modified *lysS* expression was also identified as
205 common between the B5055 and B5055Δ*wzbc* response. Our findings reveal that
206 recipient bacteria exhibit a response to conjugation that involves thematically similar

207 processes and common genes whilst also involving genes and pathways unique to each
208 recipient species.

209 **Recipient capsule inhibits donor RP4 transfer gene activation and conjugation by**
210 **blocking donor and recipient cell contact**

211 As described here and by others (19) capsules are potent inhibitors of conjugation, yet the
212 precise mechanism underlying this phenomenon remains only partially described. Our
213 earlier observations showed that capsule blocked the transcriptional response of the
214 recipient to conjugation. To determine if this effect extended to blocking the activation of
215 RP4 conjugation gene expression within the donor, additional analysis of the
216 transcriptome datasets was performed.

217 No RP4 genes were differentially expressed during conjugation with B5055 compared to
218 in the donor alone condition (Fig 2d), whilst 27 were activated during conjugation with
219 B5055Δ*wzbc* (Fig 2e), suggesting that capsule blocks RP4 gene expression in the donor
220 cell. Because the expression of RP4 genes in the B5055Δ*wzbc* mating could have
221 originated within transconjugant cells, a donor-specific fluorescent reporter assay was
222 performed to examine activity arising from the MOB promoter P*traJ* using rifampicin to
223 silence recipient transcription. This assay confirmed that MOB gene activation occurred
224 within the donor and could be blocked by recipient capsule (Supplementary Fig 3). These
225 experiments indicate that exposure to a conjugation-permissive recipient triggers RP4
226 gene expression within the donor, and can be inhibited by recipient capsule production.

227 The analysis described above also revealed that RP4 gene expression differed between
228 the conjugation-permissive recipients B5055Δ*wzbc* and DLL7555. The RP4 response to
229 DLL7555 included all genes activated by B5055Δ*wzbc* (Fig 2f), but was also broader, with
230 activation of the MPF *trb* operon detected (Fig 1d), which was not observed during
231 conjugation with B5055Δ*wzbc* (Fig 2e). Thus, RP4 gene expression is shaped by both
232 recipient species and surface structures, such as capsule.

233 Finally, to gain mechanistic insight into how capsule exerted its anti-conjugation effect,
234 imaging studies were performed to visualize the impact of *K. pneumoniae* capsule on
235 donor and recipient cell-to-cell interactions. Transmission and scanning electron

236 microscopy showed capsulated recipients localized within the donor periphery, but they
237 were physically prevented from direct outer membrane contact with the donor due to a
238 barrier formed by their capsules (Fig 2g, top panels). In contrast, direct donor and recipient
239 outer membrane contact was evident with the unencapsulated B5055Δ*wzb* (Fig 2g,
240 bottom panels). Unexpectedly, the electron microscopy imaging also revealed variation in
241 the thickness and architecture of the B5055 capsule at the single cell level, which is
242 described in detail below (Fig 3).

243 The reduced cell-to-cell contact caused by capsule appeared to block the conjugation
244 process, which was confirmed *via* fluorescence microscopy of conjugations on agarose
245 pads (Fig 2h). In these experiments, a mobilizable plasmid encoding GFP was used to
246 track conjugation to recipient cells counter-labelled with BFP on a non-mobilizable
247 plasmid. With the unencapsulated B5055Δ*wzbc* recipient, 70% of donor-contacting
248 recipient cells became transconjugants (369 transconjugants from 527 potential mating
249 pairs), indicating that direct cell-to-cell contact was highly productive for conjugation (Fig
250 2h, left panel). Conversely, with B5055 only 0.58% of donor-contacting recipient cells
251 formed transconjugants (2 transconjugants from 345 potential mating pairs), and mating
252 pairs were observed less frequently because capsule prevented direct donor and recipient
253 contact (Fig 2h, right panel). Notably, B5055 cells also showed limited contact with each
254 other, indicating that capsule reduces both intra- and inter-cellular contact.

255 Taken together, our transcriptomic and imaging data reveal that recipient capsule blocks
256 conjugation by preventing donor and recipient outer membrane contact, thereby inhibiting
257 mating pair formation and the activation of conjugation genes within the donor.

258 **RP4 exploits variation in capsule thickness and expression to overcome capsule as**
259 **a barrier to conjugation**

260 During the earlier imaging experiments, variation in *K. pneumoniae* capsular thickness at
261 the single cell level was unexpectedly observed, which prompted further characterization
262 of the *K. pneumoniae* capsule by both SEM and TEM (Fig 3).

263 SEM imaging showed capsule formed a complex, diffuse covering of the cell surface which
264 connected adjacent cells through thick projections (Fig 3a). These projections were

265 between 0.5 μm and 4 μm in length, and present within 86% of cells (581/676). The
266 majority of *K. pneumoniae* cells exhibited a complex capsular architecture, but
267 occasionally individual cells with a simple and smooth surface were observed. Under TEM,
268 capsule appeared as a diffuse, occasionally non-uniform layer which varied considerably
269 in thickness between individual cells (Fig 3b-c).

270 Total capsular diameter, i.e. the combined thickness on both sides of the cell, was
271 assessed both within and between biological replicates (Fig 3d). Across replicates, the
272 mean total capsular diameter was 287 nm and ranged from 132.8 nm to 678.8 nm,
273 reflecting considerable variation at the single cell level. Unexpectedly, capsule thickness
274 differed significantly between replicates grown and treated identically, with mean values
275 of 420.2 nm, 192.7 nm, and 263.3 nm (Fig 3d). Overall, these results demonstrate that *K.*
276 *pneumoniae* has considerable phenotypic capsular heterogeneity within clonal
277 populations.

278 Further experiments were performed to determine if variation in recipient capsule
279 thickness was the mechanism through which the small number of B5055 transconjugants
280 that normally arise during RP4 conjugation were formed. Since capsule inhibited
281 conjugation by blocking cell-to-cell contact (Fig 2g-h), it was hypothesized that recipients
282 with thin capsules could form tighter contact with donor cells, leading to effective
283 conjugation.

284 In support of this hypothesis, TEM and SEM visualisation of conjugations revealed that
285 thin-capsulated B5055 recipients formed much closer associations with the donor than did
286 thick-capsulated ones (Fig 3 e-f). Indeed, capsule thickness correlated strongly with the
287 distance between donor and recipient outer membranes (Fig 3g, $R2=0.72$, $N=47$, F test
288 $P<0.0001$), meaning that thicker capsules corresponded to a greater distance between
289 donor and recipient. Importantly, live cell fluorescence microscopy confirmed that B5055
290 transconjugants arose from recipients which could form intimate direct contact with donor
291 cells (Fig 3h). These B5055 transconjugant cells were arranged in tightly packed clusters
292 that bore a striking morphological resemblance to B5055Δ*wzbc* capsule mutants (Fig 3h,
293 inset), supporting that they were thin-capsulated.

294 Earlier, significant variation in capsule thickness was shown to occur between replicates
295 grown exactly the same way (Fig 3d). It was therefore hypothesized that variation in
296 capsule thickness between replicates would occasionally yield higher conjugation
297 frequencies for the B5055 recipient. To examine this hypothesis, numerous independent
298 conjugation experiments were performed, with the expectation that variation in capsule
299 thickness would vary between replicates, thus influencing conjugation efficiency. Of 19
300 conjugations, 4 had a mean transfer frequency of $4.2 \times 10^{-2}$ (Fig 4A). This value was ~50-
301 fold higher than the median value for the combined conjugations, but still 20-fold lower
302 than the B5055Δ*wzbc* recipient (Fig 4a), indicating that the strains were not completely
303 free of capsule. The resulting transconjugants were mucoid and string-test positive,
304 confirming that they were not spontaneous acapsular mutants.

305 RNA-seq was used to examine RP4 gene expression and recipient capsule synthesis
306 expression in the high-frequency conjugations compared to the earlier, low-frequency
307 dataset (See Fig 2). RP4 gene expression in the high frequency conjugations resembled
308 that observed with unencapsulated B5055Δ*wzbc,* in which genes for DNA mobilisation but
309 not mating pair formation were increased in expression (Fig 4b), suggesting that this is a
310 common RP4 expression pattern in conjugation-permissive *K. pneumoniae* matings.

311 Importantly, there was greatly reduced expression of principle capsule synthesis genes
312 under the control of P*wzi in* the samples that had a high conjugation frequency (Fig 4c).
313 Genes from this operon with reduced expression included *wza, wzb, wzc,* J6T75_19265*,*
314 J6T75_19270, J6T75_19275, *wzy, wzx, orf12, orf13,* and *wcaJ*. No differentially
315 expressed genes from the minor capsule synthesis operons controlled by P*galF* and
316 P*manC* were identified. A large number of additional genes contribute to capsule synthesis
317 in *K. pneumoniae* (20) and 13 of these were differentially expressed including the key
318 capsule synthesis regulator *kvrA* (21), and a variety of other regulatory and structural
319 genes, including *hha, ompR, pitA, miaA, arnD, ackA, wabH, rcsF, wabN, wcaG, fis, rfaH*
320 and *mlaF* (Fig 4d). Many other genes of diverse function were also differentially
321 expressed.

322 Lastly, because capsule serotypes have variable capsule thickness and expression, the
323 impact of this natural capsule variation on conjugation was examined. Capsule caused a

31-fold reduction in conjugation frequency with a hypermucoid K1 recipient, but a 3.3 and 2.2-fold reduction for two other hypermucoid K5 recipients compared to their parental wildtype, suggesting that differences in capsule between serotypes modulate the effect of capsule on conjugation at a strain level (Fig 4e).

Collectively, these experiments reveal an unexpected role for dynamic variation in the production of recipient capsule in determining the expression of RP4 encoded genes and conjugation frequency. These findings indicate that while recipient surface factors can greatly modulate the rate of conjugation, RP4 donor cells can exploit natural variation in these factors to permit the entry of plasmid DNA into otherwise non-permissive recipients.

**Discussion**

We investigated how recipient species and surface structures impact conjugation and the early transcriptional dynamics of the recipient and plasmid. Transcriptomic analysis of actively conjugating populations revealed a substantial recipient response in conjugation-permissive *E. coli* involving stress, motility, colanic acid production, respiratory, and metabolic pathways, alongside global RP4 gene activation (Fig 1). In contrast, *K. pneumoniae* exhibited a markedly attenuated response, and notably failed to trigger donor RP4 gene expression. Capsule disruption restored both RP4 gene activation and conjugation, leading to a recipient response with partial overlap to that of *E. coli* (Fig 2). Mechanistically, imaging revealed that capsule prevented conjugation by acting as a physical barrier to donor-recipient contact (Fig 2gh). Surprisingly, we discovered that single-cell variation in recipient capsule thickness could be exploited by the donor to facilitate RP4 entry into otherwise recalcitrant populations (Fig 3), shaping both RP4 gene expression and conjugation frequency (Fig 4).

An important finding of this work is that active conjugation triggers an immediate reshaping of the recipient transcriptome to an extent much greater than previously thought. Previous work had shown minor induction of the SOS response well after RP4 conjugation had finalized (8), but this was not detectable in two distinct recipients during early conjugation. Instead, we found that recipients express mixed stress adaptations in response to RP4 conjugation, suggesting that conjugation is detected as a potentially harmful stimulus.

355 Unexpectedly, we discovered that conjugation triggered the activation of anaerobic
356 respiration genes in both *E. coli* and *K. pneumoniae*, which were particularly upregulated
357 by *E. coli*. Both strains also exhibited differing metabolic pathway activation that in *K.*
358 *pneumoniae* was dominated by carbohydrate metabolism and in *E. coli* involved inorganic
359 nutrient metabolism. The variable impact of RP4 acquisition on metabolic pathway
360 adaptation is consistent with prior studies on plasmid metabolic reprogramming which
361 shows a high degree of dependence on host and plasmid identity (15, 22, 23). These
362 differences may arise from the unique metabolic programs of each host and reflect
363 different adaptations to meet increased energetic and stress demands post-conjugation.
364
365 10% of the recipient response was common between *E. coli* and *K. pneumoniae*, and two
366 shared genes, *ompW* and *nhaA*, reduce conjugation when deleted in recipient bacteria
367 (10, 13). OmpW is a porin involved in the transition from aerobic to anaerobic growth (24),
368 and NhaA plays a central role in maintaining sodium ion, pH, and osmotic homeostasis
369 (25). OmpW contributes to conjugation by serving as a receptor for mating pair
370 stabilization proteins, which RP4 notably does not encode. However, it is possible that the
371 common induction of *ompW* expression across two distinct recipient species might have
372 favored the evolution of mating pair stabilization systems that target OmpW. The function
373 of NhaA in conjugation is unknown, but it may protect the integrity of the recipient
374 membrane following the cell wall shock caused by conjugation as NhaA plays an essential
375 role in maintaining cellular envelope integrity (26).
376
377 Aspects of the *E. coli* response involving colanic acid and flagella production resemble the
378 establishment of a biofilm, which was perhaps not surprising as conjugation can trigger
379 biofilm formation (27). Unexpectedly, however, co-culture with the donor caused a minor
380 reduction in biofilm formation compared to the mock donor or monoculture
381 (Supplementary Fig 1), which was supported by decreased expression of a key biofilm
382 regulator *csgD*. This result suggests that the mixed-stress response induced by RP4 is
383 not a biofilm formation signal, but a distinct, and novel, process.
384
385 Our approach of examining the recipient response as conjugation actively occurred
386 enabled new insights into flagella expression following plasmid acquisition to be gained.

387 Plasmid carriage often corresponds with silencing of flagella expression (7, 23), which our
388 results suggest may occur as a compensatory measure to control flagella biosynthesis
389 triggered by conjugation itself. This suggestion explains the contradictory expression
390 pattern observed, whereby increased expression of flagella biosynthesis genes was
391 paired with decreased expression of the flagellar master activator *flhD*, and increased
392 expression of the flagella anti-sigma factor *flgM*. This may be caused by RP4 encoded
393 factors that suppress flagella production, perhaps to reduce movement of the recipient
394 away from the donor. Alternatively, RP4 may increases host cell motility to overcome
395 population structures which are barriers to RP4 dissemination (28), which the host
396 attempts to suppress through altered FlhD and FlgM production.
397
398 While conjugation can cause substantial alteration to the recipient transcriptome,
399 recipients can be shielded from this reprogramming by the production of capsule (Fig 2).
400 This protective mechanism could be beneficial in environmental contexts where a sudden
401 change in transcriptional expenditure might be detrimental to the cell, such as in a
402 mammalian host. Perhaps other surface structures serve a similar role during conjugation;
403 indeed, it is possible that the increased expression of colanic acid in DLL7555 occurred to
404 achieve a similar outcome, albeit unsuccessfully.
405
406 Although capsules have previously been reported to block conjugation (12, 29), the
407 mechanism underpinning this effect has not been fully described, nor has the significance
408 of capsule for the recipient response. Prior genetic evidence had suggested capsule was
409 too thick for the IncP pilus to cross (19), though the physical effect of capsule on
410 conjugation was not examined. By imaging conjugations through both electron and
411 fluorescence microscopy, we show that capsule forms a physical barrier that prevents
412 essential contact between donor and recipient, that in turn inhibits productive mating pair
413 formation (Fig 2). Indeed, with an average thickness of 143 nm, capsule was rarely thicker
414 than the well-characterized length the RP4 pilus, 0.2-1 μm (30-32).
415
416 Importantly, this finding was built upon further through the discovery that capsule prevents
417 RP4 gene activation in the donor (Fig 2, supplementary Fig 3). This suggests that capsule
418 obscures a component of the recipient outer membrane that triggers RP4 to begin

419 conjugation. Because RP4 can conjugate across all domains of life (33), and no non-
420 essential recipient genes are known to be necessary for conjugation, the signal is likely to
421 be a common membrane lipid that cannot be deleted. This hypothesis aligns well with the
422 fact that the lumen of conjugative pili is lined with lipids (34), and perhaps changes in pilus
423 lipid composition following their merger with the recipient outer membrane provide the
424 signal for DNA transfer.
425
426 Although recipient contact can trigger the expression of the pilus in plasmid R388 (35), the
427 pilus of RP4 is constitutively expressed (36), and we did not identify increased expression
428 of pilus-related genes during conjugation with unencapsulated *K. pneumoniae*. However,
429 pilus-related genes were activated with *E. coli*, suggesting that the recipient host
430 influences the expression of RP4 encoded genes. The basis of this phenotype is unclear
431 but could be due to the presence of co-resident plasmids within the strain of *K.*
432 *pneumoniae* used in these studies. The presence of these resident plasmids may also
433 explain why *K. pneumoniae* exhibited a smaller response to RP4 conjugation, as their
434 presence might modulate how the host responds to the acquisition of additional plasmids,
435 as for example *psiB* of the F plasmid which inhibits SOS activation (14).
436
437 An unexpected finding of this work was that stochastic variation in recipient capsule
438 thickness enabled RP4 to overcome capsule as a barrier to conjugation (Fig 3-4). This
439 was observed both at the single cell level (Fig 3) and at the level of independently grown
440 bacterial cultures (Fig 4). This finding indicates that dynamic variation in capsule can
441 greatly alter the entry of genes into recipient bacterial populations. Although these findings
442 agree with previous reports that artificially swapping capsule serotypes can change
443 conjugation frequencies (19), they also present a new perspective because they reveal
444 how natural and dynamic changes in capsule expression can allow RP4 to overcome
445 structural barriers to conjugation. The impact of single cell heterogeneity on gene transfer
446 is not yet well described but heterogeneity has been described for donor conjugation gene
447 expression, showing that MPF expression differs between individual donor cells (37). Our
448 study adds to this growing understanding of how conjugation functions between individual
449 cells within a population by showing how recipient single-cell heterogeneity in surface
450 architecture can shape gene transfer.

The cause of capsular heterogeneity studied here is unknown, but capsular heterogeneity is common within many bacterial species (38-40). One mechanism through which capsule variation occurs, phase variation (40), has long been associated with bacterial adaptation to new environments such as during host colonisation by *Neisseria meningitidis* (41). However, single cell and population heterogeneity in capsule thickness can occur by mechanisms other than phase variation, and only recently has the impact of this form of variation on natural bacterial populations begun to be understood (42). Capsule expression in *K. pneumoniae* is coordinated by multiple complex regulatory networks involving more than 70 genes (20, 43), and is mostly not phase variable (20, 44, 45). Our data suggest that the capsule variation we observe is stochastic, as there was no discernible pattern associated with its expression. However, our data raise the hypothesis that environments which alter capsule expression can shift the frequency of conjugation by modulating recipient susceptibly to conjugative plasmids.

Collectively, our findings provide new insights into how conjugation impacts recipient cell populations, and in turn how they shape conjugation. RP4 plasmid conjugation rapidly modifies the transcriptional landscape of the recipient, but its gene expression is also influenced by recipient identity and, critically, surface structures. Indeed, capsule functions not only as a modulator of physical contact but also of the early transcriptional response of the recipient. Furthermore, the unexpected discovery of stochastic capsule variation within *K. pneumoniae* reveals a novel mechanism by which gene transfer can occur in otherwise recalcitrant recipients. We determined that the early stages of conjugation are transcriptionally intensive and stressful for recipients beyond the SOS response, and that seemingly minor variations in recipient surface structures can have profound consequences for plasmid establishment within bacterial communities. Our findings have important implications for the evolution of traits which are widely disseminated by conjugation, including antibiotic resistance, virulence determinants, and metabolic pathways.

483 ## Materials and Methods

484

485 **Bacterial strains, plasmids, and growth conditions**

486 Table 1 lists the bacterial strains and plasmids used in this work. For routine growth, *E.*
487 *coli* and *K. pneumoniae* strains were cultured in low-salt LB at 37˚C shaking in liquid at
488 200 rpm or on solid media. Media was supplemented with antibiotics where necessary:
489 Ampicillin (100 µg $ml^{-1}$), rifampicin (150 µg $ml^{-1}$), erythromycin (150 µg/ml), spectinomycin
490 (50 µg/ml) and tetracycline (10 µg $ml^{-1}$).

491 **Strain and plasmid construction**

492 Prior to use as recipients, wildtype and Δ*wzbc K. pneumoniae*, along with *E. coli* DLL7555,
493 were electroporated with the low copy number vector pWSK29 to provide an ampicillin counter
494 selection maker for conjugation. Fluorescent reporter plasmids were made as follows.
495 *GFPmut3* or *mTagBFP2* were fused to a synthetic *em7* promoter (46) and synthesised as
496 gBlocks (IDT). These were cloned into the XbaI and BamHI site of pMMB67EH or pSU18
497 respectively through restriction digestion cloning. pWSK29P*traJ*GFPx3 was similarly
498 constructed, except that three translationally coupled copies of *mGreenLantern* were fused to
499 a 367 bp region upstream of the *traJ* start codon. Each *mGreenLantern* subunit was
500 independently codon optimised until each shared < 80% sequence homology.

501 **Conjugation assays**

502 Overnight liquid cultures of donor and recipient were diluted 1:50 in fresh LB and grown
503 for 4 hours before being washed once in PBS and normalized to an $OD_{600}$ 1.0. 500 µl of
504 donor and recipient culture was passed through a 0.44 µm nitrocellulose membrane filter
505 (Whattman) and incubated on LB agar at 37°C for 15 minutes before extraction in 2 ml of
506 PBS by vigorous vortexing. 15 minutes was chosen as a timepoint to prevent secondary
507 transmission of plasmid RP4, and to minimize growth of the recipient which can skew
508 transfer frequencies. For routine assays, recipient and transconjugant CFU/ml were
509 quantified by plating onto ampicillin, and ampicillin + tetracycline respectively. For *A.*
510 *baumannii*, transconjugants were quantified on ampicillin + erythromycin, and for *P.*
511 *multocida* kanamycin + spectinomycin using mobilizable plasmid pAL99S-*oriT* as a
512 surrogate for RP4 transfer. Conjugation frequency was calculated as the transconjugant
513 CFU/ml divided by recipient CFU/ml.

514

515 **RNA extraction and sequencing**

516 Conjugations were fixed after 15 minutes of incubation by vortexing mating filters in
517 RNAprotect (Qiagen). Fixed samples were pelleted at 13,300 RPM for 5 minutes, the
518 RNAprotect decanted and samples stored at -80°C for later processing. RNA was
519 extracted from the DLL7555 samples using an RNeasy RNA extraction kit (Qiagen) as per
520 the manufacturer's instructions with an on-column DNase treatment (Qiagen). Due to its
521 thick capsule, RNA from *K. pneumoniae* was isolated with hot-phenol as previously
522 described (47) and further purified using an RNeasy kit with on column-DNase treatment.
523 RNA from DLL7555-related experiments was sequenced at the MHTP Medical Genomics
524 Facility at the Monash Translational Facility. Samples were quality checked by Bioanalyzer
525 (Agilent), and libraries generated using the Illumina stranded total RNA-seq protocol with
526 ribosomal RNA depletion performed using the bacterial Ribo-Zero rRNA removal kit
527 (Illumina). Sequencing was performed on an Illumina NextSeq550 on high output mode
528 with chemistry version 2.5, using the Illumina protocol 15046563 version 2. RNA from *K.*
529 *pneumoniae* related experiments was sequenced at Micromon Genomics. Samples were
530 quality checked by Fragment Analyzer (AATI) and RNA library construction performed
531 using MGI Tech MGIEasy RNA Directional Library Prep Kit V2 (1000006386). Ribosomal
532 RNA was depleted using the rRNA depletion kit bacteria (NEB). Resulting libraries were
533 sequenced on an MGIEasy MGISEQ2000RS using V2 chemistry. For all experiments,
534 samples were sequenced to a depth that would ensure least 10 million reads per isolate
535 in the sample.

536

537 **Transcriptomic analysis**

538 Prior to analysis, we assessed the suitability of our two genetically distant *E. coli* donor
539 and recipient strains for RNA-seq analysis. Genetic variation between the donor and
540 recipient was assessed using snippy version 4.6 (48) which detected >75,000 genetic
541 variants including >68,000 SNPs which were equally distributed across the recipient
542 genome (Supplementary Fig 4). This number was in line with previous single species co-
543 culture RNA-seq experiments (49). Although the two strains were sufficiently genetically
544 distinct, 53 genes that were identical between DLL7555 and HB101 were excluded from
545 the final analysis. RNA reads were aligned against a concatenated sequence of the donor

546 (accession, CP184671.1), recipient (DLL7555, accession CP186931.1 or B5055,
547 assembly GCF_024138975.1), and pVS520 sequences (CP184672.1). The sequence for
548 HB101 ($Rif^S$ version of LT101) was used as the donor sequence owing to its availability.
549 Read alignment was performed with subread version v1.5.1 (50) against the concatenated
550 sequence which discarded reads of ambiguous donor/recipient origin. >99.8% of donor
551 originating reads were filtered by this strategy for both B5055 and DLL755 matings, which
552 was assessed by alignment of RNA isolated from the donor only condition against the
553 concatenated sequence. Read counting and assignment were performed via
554 FeatureCounts (51). Differential gene expression was analysed with the Voom/Limma
555 method in Degust v4.1 (https://drpowell.github.io/degust/) with a minimum of 3 counts per
556 million reads across 3 samples. At this stage, an additional 5 genes were subsequently
557 excluded from the DLL7555 analysis due to the detection of donor originating reads which
558 were not successfully filtered earlier. Genes were considered differentially expressed if
559 they had a Log2 fold change ≥ 0.585, a P value ≤ 0.05, and an FDR ≤ 0.05. GO term
560 analysis was performed using the TopGO R package v2.58 (52), with the weight_01
561 algorithm using raw P-values due to the structured dependency of GO terms as per the
562 package guidelines. eggNOG mapper v2.1.8 (53) was used to assign GO-terms to the
563 GenBank recipient proteomes. Gene and pathway functions were also assessed using the
564 ecocyc database (54). Heatmaps and GO term plots were generated using ggplot2 v3.5.2
565 (55).
566
567 **Scanning and Transmission Electron Microscopy**
568 SEM was performed on *K. pneumoniae* cells during conjugation, or in stationary phase
569 when capsule is highly expressed(20). 500 µl of cells were collected onto a 0.4 µm
570 polycarbonate membrane, and the capsular ultrastructure preserved by lysine acetate,
571 ruthenium red and osmium (LRR) fixation (56), followed by graduated dehydration in
572 ethanol, critical point drying, and gold sputter coating as previously described (57).
573 Samples were imaged on a field emission NovaSEM 450 SEM with an acceleration
574 voltage of 10 kV in secondary electron mode with a working distance of ~4.5mm. Images
575 were taken under immersion mode through the lens detector.
576

577 For TEM imaging, cells were collected on polycarbonate membranes and prepared with
578 LRR fixation as for SEM. Fixed membranes were then cut into small rectangles no longer
579 than 1 mm cubed, dehydrated and then infiltrated with Epon resin (58). Each membrane
580 was placed on a glass slide cell-side up, and a BEEM® capsule containing 100% resin
581 positioned over the flat membrane before polymerisation at 60°C for 48 hours. The resin-
582 filled BEEM® capsule and slide were cooled in liquid nitrogen and then immediately
583 separated, leaving the flat membrane with cells in a longitudinal orientation on the surface
584 of the resin block. Cells were ultrathin sectioned using a Leica UC7 ultramicrotome and
585 Diatome diamond knife and then contrasted with uranyl acetate and lead citrate. Cells
586 were imaged on a JEOL JEM-1400 Plus TEM at 80 KeV, equipped with a high sensitivity
587 bottom mount CMOS 'Flash' camera. Total capsule diameter was measured from the
588 average of 5 total cell widths from which the cell body width was subtracted, as described
589 previously (59).
590

591 **Fluorescent Microscopy and Image analysis**

592 Conjugation was analysed by fluorescent microscopy by inoculation of 1 µl of $OD_{600}$ 0.1
593 recipient and donor onto LB 1% agarose pads. Pads were incubated in parafilm sealed 25
594 mm fluorodish chamber (WPI) for 2 hours at 37°C. Small strips of moist KimWipe® were
595 included in the chamber to prevent pad dehydration. Images were acquired using a
596 63x/1.30 oil objective on a Leica DMI-8 widefield microscope equipped with a Lecia K8
597 sCMOS monochromatic camera using Lecia LasX software. Mating pair productivity was
598 assessed by counting transconjugants that were in direct contact with a donor and dividing
599 that by the total number of recipients in contact with a donor.

600 **Fluorescent reporter assays**

601 Fluorescent measurements were taken on a Tecan infinite pro 200 plate reader. For
602 measurement of P*traJ*, 15 µl of *K. pneumoniae* was inoculated onto a 200 µl LB 1%
603 agarose pad with rifampicin in a 96-well special optics microtiter plate (Corning). After 5
604 minutes of incubation and air drying, 15 µl of donor culture was spotted on top and
605 immediately afterwards the OD600 and fluorescent intensity (488 nm / 520 nm) were
606 measured in 5-minute intervals at 37°C. Fluorescent intensity was then normalised to

OD600 and analysed as change over time by calculating fold-change against the 0-time point value.

**Acknowledgments:** We would like to acknowledge Dr Francesca Short for providing strains and protocols for RNA isolation, and Dr Tom Smallman and Prof John Boyce for providing strains. The authors acknowledge use of the facilities and the assistance of Alex Fulcher from Monash Micro Imaging. The authors acknowledge the use of instruments and assistance at the Monash Ramaciotti Centre for Cryo-Electron Microscopy, a Node of Microscopy Australia. The authors acknowledge the MHTP Medical Genomics Facility for assistance with RNA sequencing.

**Funding:** This work was supported by the Australian Research Council Grant DP250103521, and Australian Research Council Laureate Fellowship FL210100258 awarded to D.L., and funding for Y.H. Gan from the National Medical Research Council, grant number OFIRG20NOV-0045.

640 ## References


641 1. S. Castañeda-Barba, E. M. Top, T. Stalder, Plasmids, a molecular cornerstone of
642 antimicrobial resistance in the One Health era. *Nature Reviews Microbiology* **22**, 18-32
643 (2024).
644 2. C. Virolle, K. Goldlust, S. Djermoun, S. Bigot, C. Lesterlin, Plasmid Transfer by Conjugation
645 in Gram-Negative Bacteria: From the Cellular to the Community Level. *Genes (Basel)* **11**
646 (2020).
647 3. K. Billane, E. Harrison, D. Cameron, M. A. Brockhurst, Why do plasmids manipulate the
648 expression of bacterial phenotypes? *Philosophical Transactions of the Royal Society B:*
649 *Biological Sciences* **377**, 20200461 (2022).
650 4. H. Lee, K. S. Ko, Effect of multiple, compatible plasmids on the fitness of the bacterial host
651 by inducing transcriptional changes. *Journal of Antimicrobial Chemotherapy* **76**, 2528-
652 2537 (2021).
653 5. C. Huang *et al.*, Comparative Analysis of Transcriptome and Proteome Revealed the
654 Common Metabolic Pathways Induced by Prevalent ESBL Plasmids in Escherichia coli.
655 *International Journal of Molecular Sciences* **24**, 14009 (2023).
656 6. A. San Millan, M. Toll-Riera, Q. Qi, R. C. MacLean, Interactions between horizontally
657 acquired genes create a fitness cost in Pseudomonas aeruginosa. *Nature Communications*
658 **6**, 6845 (2015).
659 7. K. Schaufler *et al.*, Carriage of Extended-Spectrum Beta-Lactamase-Plasmids Does Not
660 Reduce Fitness but Enhances Virulence in Some Strains of Pandemic E. coli Lineages. *Front*
661 *Microbiol* **7**, 336 (2016).
662 8. Z. Baharoglu, D. Bikard, D. Mazel, Conjugative DNA Transfer Induces the Bacterial SOS
663 Response and Promotes Antibiotic Resistance Development through Integron Activation.
664 *PLOS Genetics* **6**, e1001165 (2010).
665 9. K. Moriguchi *et al.*, Targeting Antibiotic Resistance Genes Is a Better Approach to Block
666 Acquisition of Antibiotic Resistance Than Blocking Conjugal Transfer by Recipient Cells: A
667 Genome-Wide Screening in Escherichia coli. *Front Microbiol* **10**, 2939 (2019).
668 10. D. Pérez-Mendoza, F. de la Cruz, Escherichia coli genes affecting recipient ability in
669 plasmid conjugation: Are there any? *BMC Genomics* **10**, 71 (2009).
670 11. C. M. Johnson, A. D. Grossman, The Composition of the Cell Envelope Affects Conjugation
671 in Bacillus subtilis. *J Bacteriol* **198**, 1241-1249 (2016).
672 12. M. Haudiquet, A. Buffet, O. Rendueles, E. P. C. Rocha, Interplay between the cell envelope
673 and mobile genetic elements shapes gene flow in populations of the nosocomial
674 pathogen Klebsiella pneumoniae. *PLOS Biology* **19**, e3001276 (2021).
675 13. W. W. Low *et al.*, Mating pair stabilization mediates bacterial conjugation species
676 specificity. *Nature Microbiology* **7**, 1016-1027 (2022).
677 14. M. Al Mamun Abu Amar, K. Kishida, J. Christie Peter, Protein Transfer through an F
678 Plasmid-Encoded Type IV Secretion System Suppresses the Mating-Induced SOS
679 Response. *mBio* **12**, 10.1128/mbio.01629-01621 (2021).
680 15. L. González-Montes, I. Del Campo, M. P. Garcillán-Barcia, F. de la Cruz, G. Moncalián,
681 ArdC, a ssDNA-binding protein with a metalloprotease domain, overpasses the recipient

682 hsdRMS restriction system broadening conjugation host range. *PLoS Genet* **16**, e1008750
683 (2020).
684 16. K. H. Maslowska, K. Makiela-Dzbenska, I. J. Fijalkowska, The SOS system: A complex and
685 tightly regulated response to DNA damage. *Environ Mol Mutagen* **60**, 368-384 (2019).
686 17. M. Miyakoshi, Y. Ohtsubo, Y. Nagata, M. Tsuda, Transcriptome Analysis of Zygotic
687 Induction During Conjugative Transfer of Plasmid RP4. *Frontiers in Microbiology* **Volume**
688 **11 - 2020** (2020).
689 18. H. Prensky, A. Gomez-Simmonds, A. C. Uhlemann, A. J. Lopatkin, Conjugation dynamics
690 depend on both the plasmid acquisition cost and the fitness cost. *Molecular Systems*
691 *Biology* **17**, e9913 (2021).
692 19. M. Haudiquet *et al.*, Capsules and their traits shape phage susceptibility and plasmid
693 conjugation efficiency. *Nature Communications* **15**, 2032 (2024).
694 20. M. J. Dorman, T. Feltwell, D. A. Goulding, J. Parkhill, F. L. Short, The Capsule Regulatory
695 Network of Klebsiella pneumoniae Defined by density-TraDISort. *mBio* **9** (2018).
696 21. M. Palacios *et al.*, Identification of Two Regulators of Virulence That Are Conserved in
697 Klebsiella pneumoniae Classical and Hypervirulent Strains. *mBio* **9** (2018).
698 22. J. Hall Rebecca, E. Snaith Ann, J. N. Thomas Matthew, A. Brockhurst Michael, A. McNally,
699 Multidrug resistance plasmids commonly reprogram the expression of metabolic genes
700 in Escherichia coli. *mSystems* **9**, e01193-01123 (2024).
701 23. L. Toribio-Celestino *et al.*, A plasmid-chromosome crosstalk in multidrug resistant
702 enterobacteria. *Nature Communications* **15**, 10859 (2024).
703 24. M. Xiao, Y. Lai, J. Sun, G. Chen, A. Yan, Transcriptional Regulation of the Outer Membrane
704 Porin Gene ompW Reveals its Physiological Role during the Transition from the Aerobic
705 to the Anaerobic Lifestyle of Escherichia coli. *Front Microbiol* **7**, 799 (2016).
706 25. T. A. Krulwich, G. Sachs, E. Padan, Molecular aspects of bacterial pH sensing and
707 homeostasis. *Nat Rev Microbiol* **9**, 330-343 (2011).
708 26. Z. Mao *et al.*, NhaA facilitates the maintenance of bacterial envelope integrity and the
709 evasion of complement attack contributing to extraintestinal pathogenic Escherichia coli
710 virulence. *Infect Immun* **91**, e0003923 (2023).
711 27. J. M. Ghigo, Natural conjugative plasmids induce bacterial biofilm development. *Nature*
712 **412**, 442-445 (2001).
713 28. S. Djermoun *et al.*, Biofilm architecture determines the dissemination of conjugative
714 plasmids. *Proceedings of the National Academy of Sciences* **122**, e2417452122 (2025).
715 29. M. Yong *et al.*, Dominant Carbapenemase-Encoding Plasmids in Clinical Enterobacterales
716 Isolates and Hypervirulent Klebsiella pneumoniae, Singapore. *Emerg Infect Dis* **28**, 1578-
717 1588 (2022).
718 30. G. Schröder, E. Lanka, The mating pair formation system of conjugative plasmids—A
719 versatile secretion machinery for transfer of proteins and DNA. *Plasmid* **54**, 1-25 (2005).
720 31. W. Pansegrau, E. Lanka, Enzymology of DNA Transfer by Conjugative Mechanisms.
721 *Progress in Nucleic Acid Research and Molecular Biology* **54**, 197-251 (1996).
722 32. J. Haase, R. Lurz, A. M. Grahn, D. H. Bamford, E. Lanka, Bacterial conjugation mediated by
723 plasmid RP4: RSF1010 mobilization, donor-specific phage propagation, and pilus
724 production require the same Tra2 core components of a proposed DNA transport
725 complex. *Journal of Bacteriology* **177**, 4779-4791 (1995).

726 33. S. Bates, A. M. Cashmore, B. M. Wilkins, IncP plasmids are unusually effective in mediating
727 conjugation of Escherichia coli and Saccharomyces cerevisiae: involvement of the tra2
728 mating system. *J Bacteriol* **180**, 6538-6543 (1998).
729 34. T. R. D. Costa, J. B. Patkowski, K. Macé, P. J. Christie, G. Waksman, Structural and
730 functional diversity of type IV secretion systems. *Nature Reviews Microbiology* **22**, 170-
731 185 (2024).
732 35. A. K. Vadakkepat *et al.*, Cryo-EM structure of the R388 plasmid conjugative pilus reveals
733 a helical polymer characterized by an unusual pilin/phospholipid binary complex.
734 *Structure* 10.1016/j.str.2024.06.009.
735 36. D. E. Bradley, Morphological and serological relationships of conjugative pili. *Plasmid* **4**,
736 155-169 (1980).
737 37. V. Cyriaque *et al.*, Single-cell RNA sequencing reveals plasmid constrains bacterial
738 population heterogeneity and identifies a non-conjugating subpopulation. *Nature*
739 *Communications* **15**, 5853 (2024).
740 38. S. E. George *et al.*, Phenotypic heterogeneity and temporal expression of the capsular
741 polysaccharide in Staphylococcus aureus. *Molecular Microbiology* **98**, 1073-1088 (2015).
742 39. J. E. King, H. A. Aal Owaif, J. Jia, I. S. Roberts, Phenotypic Heterogeneity in Expression of
743 the K1 Polysaccharide Capsule of Uropathogenic Escherichia coli and Downregulation of
744 the Capsule Genes during Growth in Urine. *Infect Immun* **83**, 2605-2613 (2015).
745 40. L. M. Reyes Ruiz, C. L. Williams, R. Tamayo, Enhancing bacterial survival through
746 phenotypic heterogeneity. *PLOS Pathogens* **16**, e1008439 (2020).
747 41. S. Hammerschmidt *et al.*, Capsule phase variation in Neisseria meningitidis serogroup B
748 by slipped-strand mispairing in the polysialyltransferase gene (siaD): correlation with
749 bacterial invasion and the outbreak of meningococcal disease. *Mol Microbiol* **20**, 1211-
750 1220 (1996).
751 42. J. Zhu *et al.*, Effects of Capsular Polysaccharide amount on Pneumococcal-Host
752 interactions. *PLOS Pathogens* **19**, e1011509 (2023).
753 43. K. A. Walker, V. L. Miller, The intersection of capsule gene expression, hypermucoviscosity
754 and hypervirulence in Klebsiella pneumoniae. *Current opinion in microbiology* **54**, 95-102
755 (2020).
756 44. M. A. Schembri, J. Blom, K. A. Krogfelt, P. Klemm, Capsule and fimbria interaction in
757 Klebsiella pneumoniae. *Infect Immun* **73**, 4626-4633 (2005).
758 45. D.-W. Wei *et al.*, Insertion sequences accelerate genomic convergence of multidrug
759 resistance and hypervirulence in Klebsiella pneumoniae via capsular phase variation.
760 *Genome Medicine* **17**, 45 (2025).
761 46. S. Zobel *et al.*, Tn7-Based Device for Calibrated Heterologous Gene Expression in
762 Pseudomonas putida. *ACS Synthetic Biology* **4**, 1341-1351 (2015).
763 47. N. R. Mattatall, K. E. Sanderson, Salmonella typhimurium LT2 possesses three distinct 23S
764 rRNA intervening sequences. *Journal of Bacteriology* **178**, 2272-2278 (1996).
765 48. T. Seemann, Snippy: rapid haploid variant calling and core SNP phylogeny. *GitHub.*
766 *Available at: github. com/tseemann/snippy* (2015).
767 49. T. A. Gray *et al.*, Intercellular communication and conjugation are mediated by ESX
768 secretion systems in mycobacteria. *Science* **354**, 347-350 (2016).

50. Y. Liao, G. K. Smyth, W. Shi, The Subread aligner: fast, accurate and scalable read mapping by seed-and-vote. *Nucleic Acids Res* **41**, e108 (2013).
51. Y. Liao, G. K. Smyth, W. Shi, featureCounts: an efficient general purpose program for assigning sequence reads to genomic features. *Bioinformatics* **30**, 923-930 (2014).
52. A. Alexa, J. Rahnenführer, Gene set enrichment analysis with topGO. *Bioconductor Improv* **27**, 776 (2009).
53. C. P. Cantalapiedra, A. Hernández-Plaza, I. Letunic, P. Bork, J. Huerta-Cepas, eggNOG-mapper v2: Functional Annotation, Orthology Assignments, and Domain Prediction at the Metagenomic Scale. *Molecular Biology and Evolution* **38**, 5825-5829 (2021).
54. P. D. Karp *et al.*, The EcoCyc Database (2023). *EcoSal Plus* **11**, eesp-0002-2023 (2023).
55. H. Wickham, C. Sievert, *ggplot2: elegant graphics for data analysis* (springer New York, 2009), vol. 10.
56. S. Hammerschmidt, M. Rohde, "Electron Microscopy to Study the Fine Structure of the Pneumococcal Cell" in Streptococcus pneumoniae: Methods and Protocols*,* F. Iovino, Ed. (Springer New York, New York, NY, 2019), 10.1007/978-1-4939-9199-0_2, pp. 13-33.
57. T. R. Smallman, G. C. Williams, M. Harper, J. D. Boyce, Genome-Wide Investigation of Pasteurella multocida Identifies the Stringent Response as a Negative Regulator of Hyaluronic Acid Capsule Production. *Microbiology Spectrum* **10**, e00195-00122 (2022).
58. S. A. C. Jillian C Danne and Jillian C Danne, Rachel Templin, Joan Clark, Viola Oorschot, Georg Ramm, Preparation of cells for transmission electron microscopy ultrastructural analysis. *protocols.io* dx.doi.org/10.17504/protocols.io.j8nlk47ewg5r/v1 (2022).
59. T. Guess *et al.*, Size Matters: Measurement of Capsule Diameter in Cryptococcus neoformans. *JoVE* doi:10.3791/57171, e57171 (2018).
60. B. M. Coffey, G. G. Anderson, Biofilm formation in the 96-well microtiter plate. *Methods Mol Biol* **1149**, 631-641 (2014).
61. E. A. Palombo, K. Yusoff, V. A. Stanisich, V. Krishnapillai, N. S. Willetts, Cloning and genetic analysis of tra cistrons of the Tra 2/Tra 3 region of plasmid RP1. *Plasmid* **22**, 59-69 (1989).
62. Y. Fu *et al.*, Mechanisms of blaIMP-4 dissemination across diverse carbapenem-resistant clinical isolates. *Journal of Global Antimicrobial Resistance* **41**, 189-194 (2025).
63. M. M. C. Lam *et al.*, Population genomics of hypervirulent Klebsiella pneumoniae clonal-group 23 reveals early emergence and rapid global dissemination. *Nature Communications* **9**, 2703 (2018).
64. I. R. Lee *et al.*, Differential host susceptibility and bacterial virulence factors driving Klebsiella liver abscess in an ethnically diverse population. *Scientific Reports* **6**, 29316 (2016).
65. A. C. Jacobs *et al.*, AB5075, a Highly Virulent Isolate of Acinetobacter baumannii, as a Model Strain for the Evaluation of Pathogenesis and Antimicrobial Treatments. *mBio* **5**, e01076-01014 (2014).
66. L. A. Gallagher *et al.*, Resources for Genetic and Genomic Analysis of Emerging Pathogen Acinetobacter baumannii. *J Bacteriol* **197**, 2027-2035 (2015).
67. R. F. Wang, S. R. Kushner, Construction of versatile low-copy-number vectors for cloning, sequencing and gene expression in Escherichia coli. *Gene* **100**, 195-199 (1991).

811 68. B. Bartolomé, Y. Jubete, E. Martínez, F. de la Cruz, Construction and properties of a family
812 of pACYC184-derived cloning vectors compatible with pBR322 and its derivatives. *Gene*
813 **102**, 75-78 (1991).
814 69. J. P. Fürste *et al.*, Molecular cloning of the plasmid RP4 primase region in a multi-host-
815 range tacP expression vector. *Gene* **48**, 119-131 (1986).

816

## Figures and Tables

851

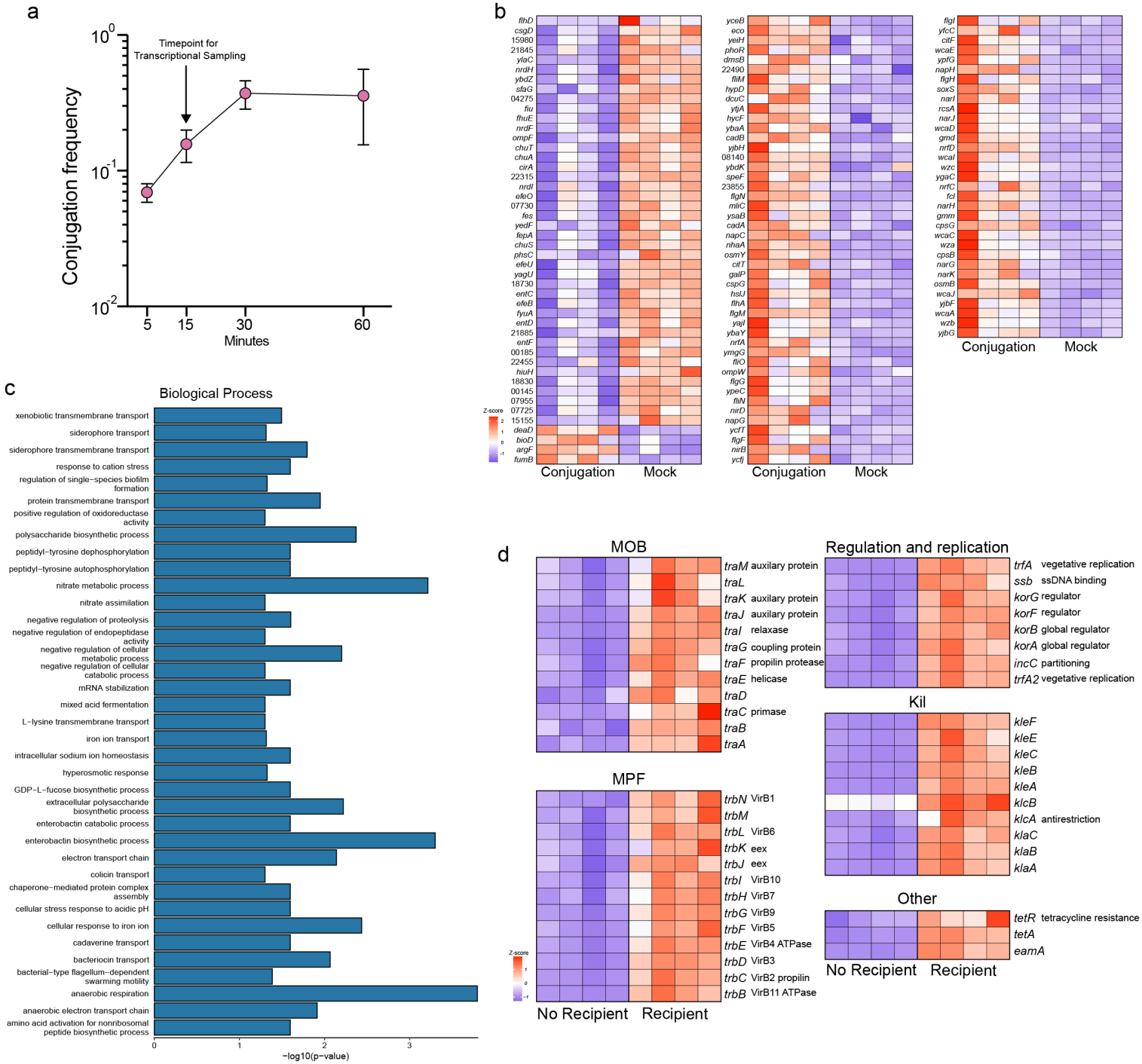


852

853

854

855 **Figure 1. The transcriptional response of an *E. coli* recipient and plasmid RP4 during active**
856 **conjugation**. **a)** *E. coli* DLL7555 conjugation frequency over time shows that RP4 conjugation is
857 active at 15 minutes and completed by 30 minutes. Arrow indicates time for transcriptional
858 sampling. **b)** Differentially expressed DLL7555 genes during active RP4 conjugation. **c)** GO term
859 analysis of enriched genes with the R TopGo package with the weight_01 algorithm. **d)** Differential
860 expression of RP4 encoded genes during active conjugation with *E. coli* DLL7555. Numbers in *E.*
861 *coli* gene list represent locus tags trimmed of the prefix ACPEGL. Error bars = mean ± SD, N = 4.
862
863

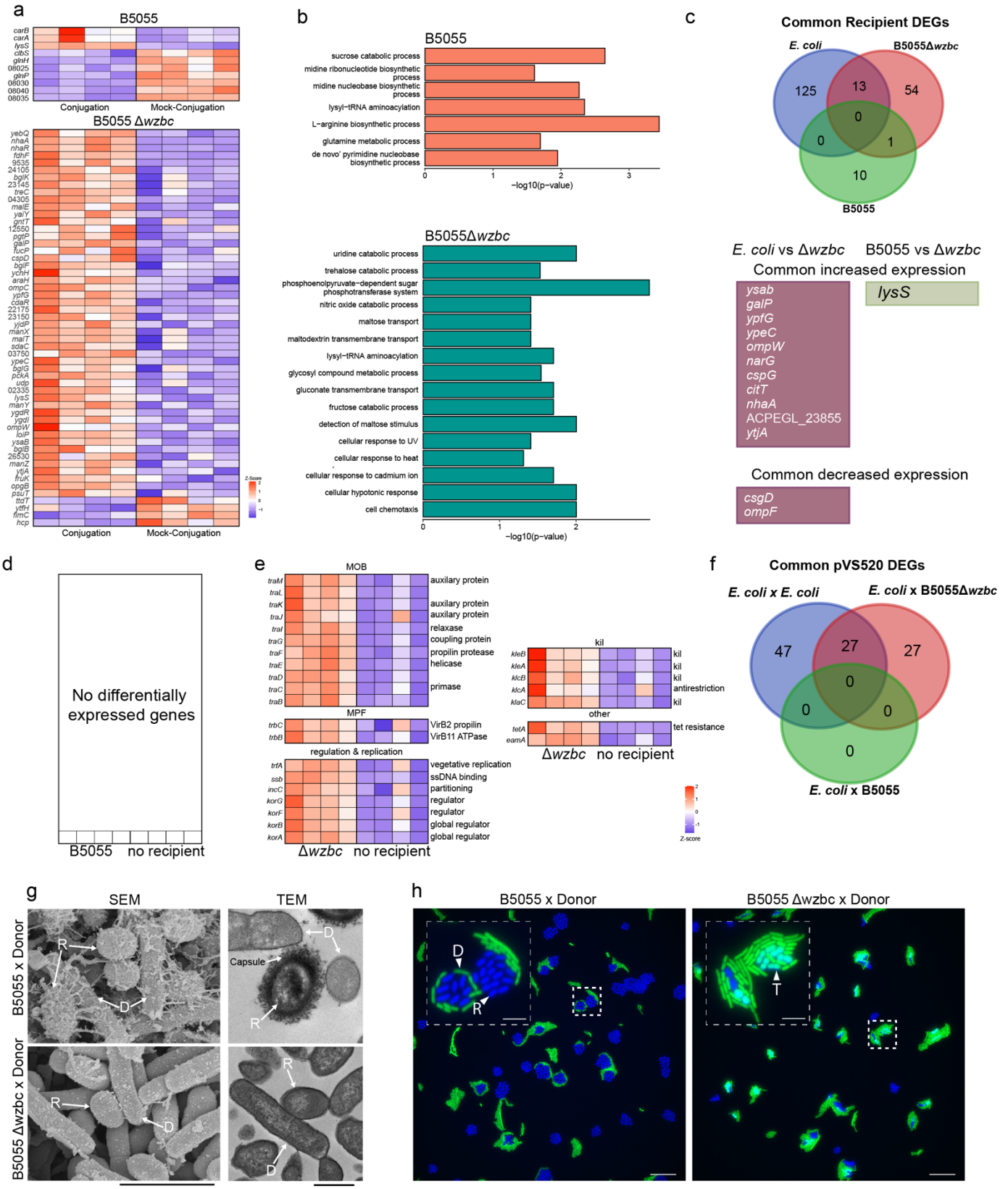
a
B5055
carB
carA
lysS
clbS
glnH
08025
glnP
08030
08040
08035
Conjugation
Mock-Conjugation
B5055 Δwzbc
yebQ
nhaA
nhaR
fdhF
9535
24105
bglK
23145
treC
04305
malE
yaiY
gntT
12550
pgtP
galP
fucP
cspD
bglF
ychH
araH
ompC
ypfG
cdaR
22175
23150
ydiP
manX
malT
sdaC
03750
ypeC
bglG
pckA
udp
02335
lysS
manY
ygdR
ygdI
ompW
loiP
ysaB
bglB
26530
manZ
ytjA
fruK
opgB
psuT
ttdT
ytfH
fimC
hcp
Z-Score
Conjugation
Mock-Conjugation
b
B5055
sucrose catabolic process
midine ribonucleotide biosynthetic process
midine nucleobase biosynthetic process
lysyl−tRNA aminoacylation
L−arginine biosynthetic process
glutamine metabolic process
de novo' pyrimidine nucleobase biosynthetic process
0
1
2
3
−log10(p−value)
B5055Δwzbc
uridine catabolic process
trehalose catabolic process
phosphoenolpyruvate−dependent sugar phosphotransferase system
nitric oxide catabolic process
maltose transport
maltodextrin transmembrane transport
lysyl−tRNA aminoacylation
glycosyl compound metabolic process
gluconate transmembrane transport
fructose catabolic process
detection of maltose stimulus
cellular response to UV
cellular response to heat
cellular response to cadmium ion
cellular hypotonic response
cell chemotaxis
0
1
2
−log10(p−value)
c
Common Recipient DEGs
E. coli
B5055Δwzbc
125
13
54
0
0
1
10
B5055
E. coli vs Δwzbc
B5055 vs Δwzbc
Common increased expression
ysab
galP
ypfG
ypeC
ompW
narG
cspG
citT
nhaA
ACPEGL_23855
ytjA
lysS
Common decreased expression
csgD
ompF
d
No differentially expressed genes
B5055
no recipient
e
MOB
traM
traL
traK
traJ
traI
traG
traF
traE
traD
traC
traB
auxilary protein
auxilary protein
auxilary protein
relaxase
coupling protein
propilin protease
helicase
primase
MPF
trbC
trbB
VirB2 propilin
VirB11 ATPase
regulation & replication
trfA
ssb
incC
korG
korF
korB
korA
vegetative replication
ssDNA binding
partitioning
regulator
regulator
global regulator
global regulator
Δwzbc
no recipient
kil
kleB
kleA
klcB
klcA
klaC
kil
kil
kil
antirestriction
kil
other
tetA
eamA
tet resistance
Δwzbc
no recipient
Z-score
f
Common pVS520 DEGs
E. coli x E. coli
E. coli x B5055Δwzbc
47
27
27
0
0
0
0
E. coli x B5055
g
SEM
TEM
B5055 x Donor
B5055 Δwzbc x Donor
R
D
Capsule
R
D
R
D
R
D
h
B5055 x Donor
B5055 Δwzbc x Donor
D
R
T

865 **Figure 2. The effect and mechanism of capsule on conjugation and the recipient and plasmid**
866 **response. a)** Differentially expressed genes (DEGS) in *K. pneumoniae* B5055 (top) and
867 B5055Δ*wzbc* (bottom) genes during active conjugation or co-culture with an RP4 donor. **b)** GO
868 term analysis of DEG for B5055 (top) and B5055Δ*wzbc*, with raw P-values reported as per TopGO
869 package guidelines for the weight_01 algorithm. **c)** Common DEGS between recipient responses
870 (top), that are increased in expression (middle) or decreased (bottom). **d)** No RP4 DEGS were
871 detected in the conjugation mixture with B5055. **e)** Differentially expressed RP4 genes during active
872 conjugation with B5055Δ*wzbc*. **f)** DEGs shared between RP4 during conjugation across different
873 recipients. **g)** TEM, and SEM images of conjugation between *K. pneumoniae* B5055 or
874 B5055Δ*wzbc* recipients with *E. coli* LT101. Recipients are distinguished based on the presence of
875 capsule, and shape. **h)** *in situ* visualisation of conjugation between either wildtype or Δ*wzbc*
876 recipients by fluorescent microscopy. All images are representative of ≥2 independent experiments.
877 Abbreviations: D=Donor, R=Recipient, T=Transconjugant. Numbers in *K. pneumoniae* gene lists
878 represent locus tags trimmed of the prefix J6T75_RS. Scale bars: SEM 3 μm, TEM 1 μm,
879 Fluorescence microscopy 20 μm, inset 5 μm.
880
881
882
883
884
885
886
887
888
889
890
891
892
893
894
895

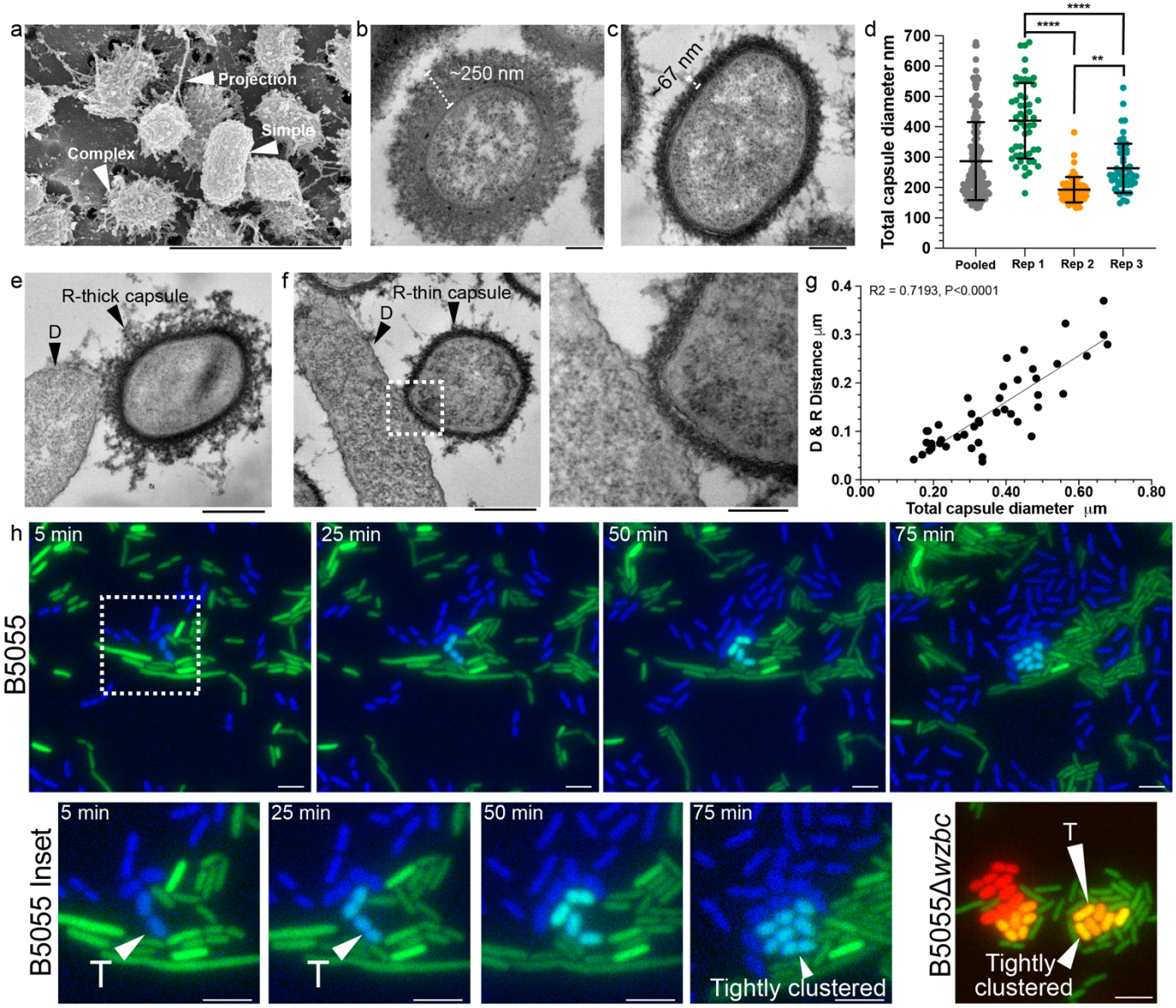


**Figure 3. Recipient *K. pneumoniae* capsule thickness variation impacts donor-recipient interactions and conjugation. a)** SEM imaging of capsular variation and projections. **b-c)** TEM imaging of capsule thickness variation between individual cells. **d)** Variation in capsule thickness within, and between biological replicates (n = ≥50 cells per sample, one-way ANOVA with sidak's multiple comparison testing P-values = ** ≤ 0.01, **** ≤ 0.0001.). **e-f)** Effect of capsule thickness variation on donor-recipient interactions. **g)** linear regression analysis of distance between outer membrane of donor and recipient and total capsular diameter ($R^2$=.72, N=47, F-test P≤0.0001). **h)**

905 live cell imaging of B5055 transconjugant formation, showing that B5055 transconjugants arise
906 from recipients intimately contacting the donor and morphologically resemble acapsular
907 B5055Δ*wzbc*. Error bars = mean ± SD. Scale bars: a = 5 μm, bc = 200 nm, ef = 500 nm, f inset =
908 200 nm, h = 20 μm, h insert = 5 μm. Images are representative of ≥ 2 independent experiments,
909 except for h which depicts the rare formation of a B5055 transconjugant.
910
911
912
913
914

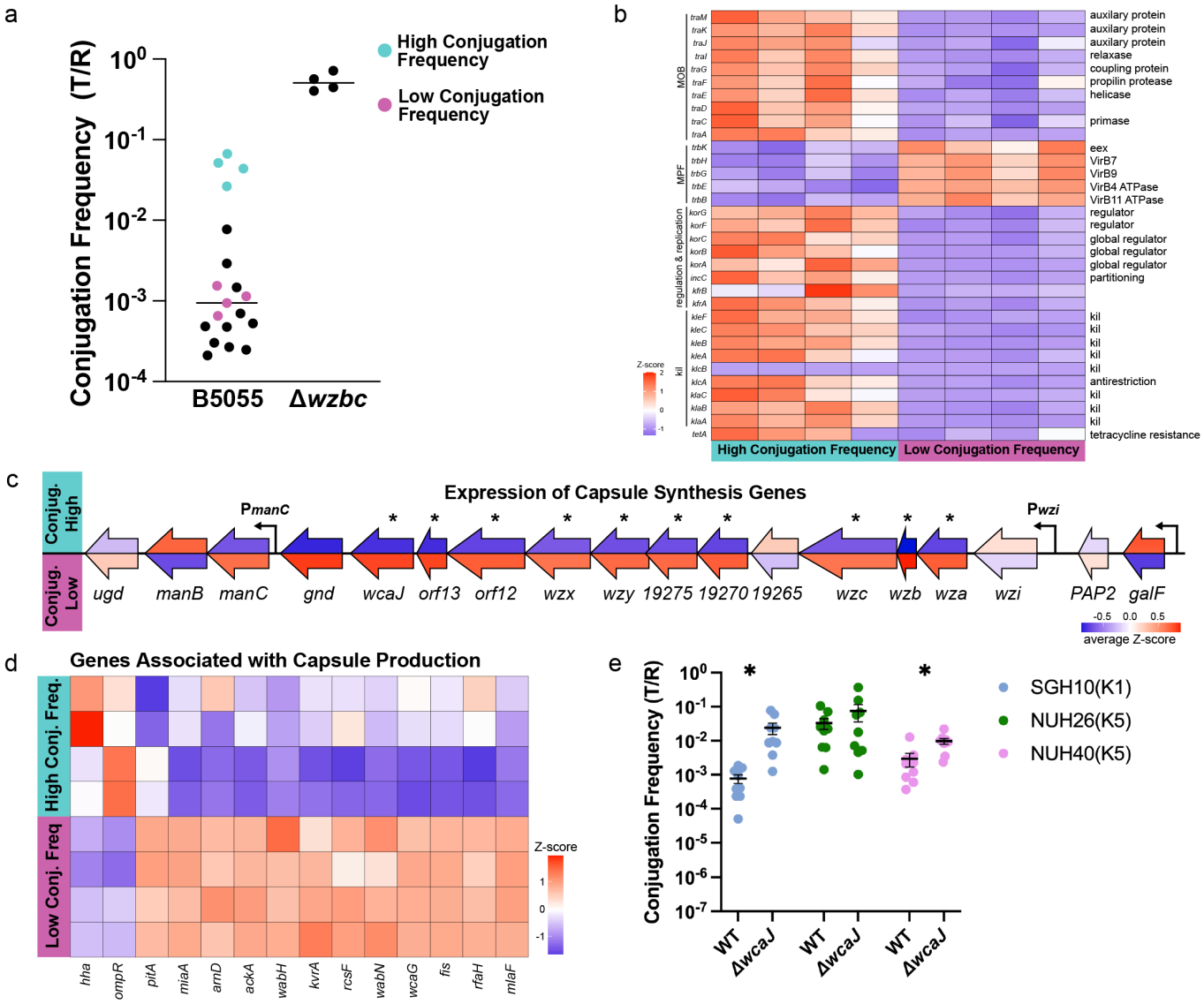


**Figure 4. Population level capsule variation enables RP4 conjugation in capsulated *K. pneumoniae*.**

**a)** Variation in conjugation frequency of *K. pneumoniae* B5055. The conjugation frequency of B5055Δ*wzbc* is shown for context. **b)** Differential expression of RP4 encoded genes between conjugation high and low samples. **c)** differential expression of genes in the capsule synthesis locus between conjugation high (top) and low (bottom) samples. **d)** Genes associated with capsule production between samples with high or low conjugation frequencies. **e)** The

923 conjugation frequency of RP4 to hypermucoid K1 or K5 *K. pneumoniae* (N=9, P>.05 Mann-
924 Whitney U test). Data are presented as the median (**a**), or the mean+SEM (**d**).

925

926

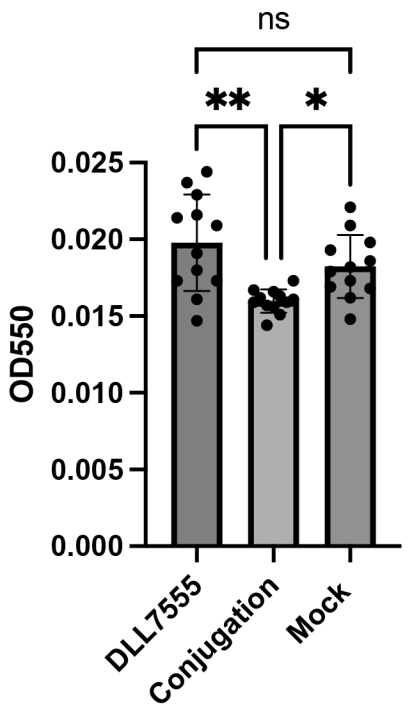


927

928

929 **Supplementary Figure 1: Donor LT101(pVS520) and Recipient DLL7555 co-culture causes a**
930 **minor reduction in biofilm formation.**
931 Biofilms were grown as in (60). Briefly, 1:100 dilutions of overnight broth cultures of donor, recipient
932 and mock donor in fresh LB medium were mixed in 1:1 in a flat bottomed 96 well tray and grown
933 for 24 hours at 37°C. Outer wells were not used to avoid evaporation effects. Following incubation,
934 the liquid portion of the culture was removed and plated to confirm transconjugants were present
935 and therefore conjugation had occurred. The biofilms were washed in water, and quantitated by
936 staining with 0.1% crystal violet, which after washing was solubilized with 30% acetic acid and
937 measured by absorbance reading at 550 nm standardized against 30% acetic acid. Error bars =
938 mean ± SD, N = 4 biological replicates repeated 3 times). Significance testing was performed with
939 a Kruskal Wallis one way ANOVA with Dunn's multiple comparison testing P-values = *** ≤ 0.01,
940 **** ≤ 0.0001.).

941

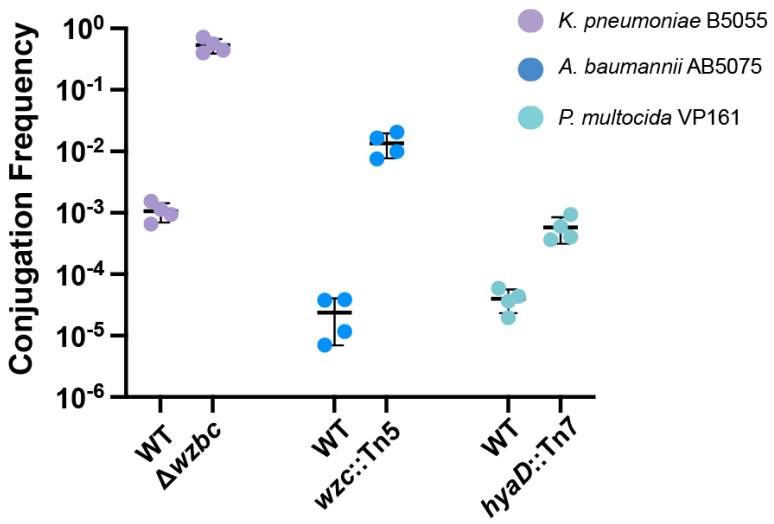


**Supplementary Figure 2: Capsule is a barrier to conjugation in diverse species.**
The conjugation frequency of RP4 or RP4-mobilizable plasmids from *E. coli* LT101 to K. *pneumoniae* B5055, *A. baumannii* AB5075, or *P. multocida* VP161 and their unencapsulated derivatives (Mean+SD, N=4, P>.05 Mann-Whitney U test).

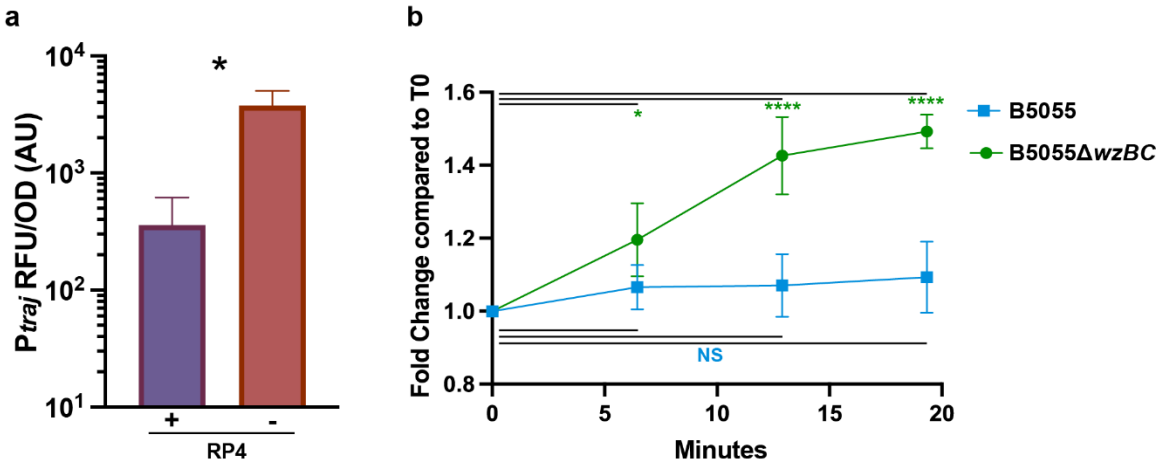


**Supplementary Figure 3: Capsule inhibits activation of the RP4 MOB promoter P*traJ* within the donor.** We constructed a fluorescent reporter for the RP4 MOB promoter P*traJ* by fusing it to three tandem low sequence-homology GFP reporters. Three tandem GFPs were used because fluorescence from 1 GFP reporter could not be detected, likely because P*traJ* is a weak promoter **a)** we confirmed our reporter behaved as expected by comparing expression in the presence or absence of RP4, which is known to repress P*traJ* activity (N = 4, P<0.05, Mann-Whitney U-Test). **b)** Measurement of P*traJ*x3GFP in the donor cell was achieved by performing conjugations in a 96-well tray on agar containing rifampicin which inhibits transcription only in the recipient cell. Significance testing was performed with a one-way ANOVA with Sidak's multiple comparison. Error bars = mean ± SD

974

a

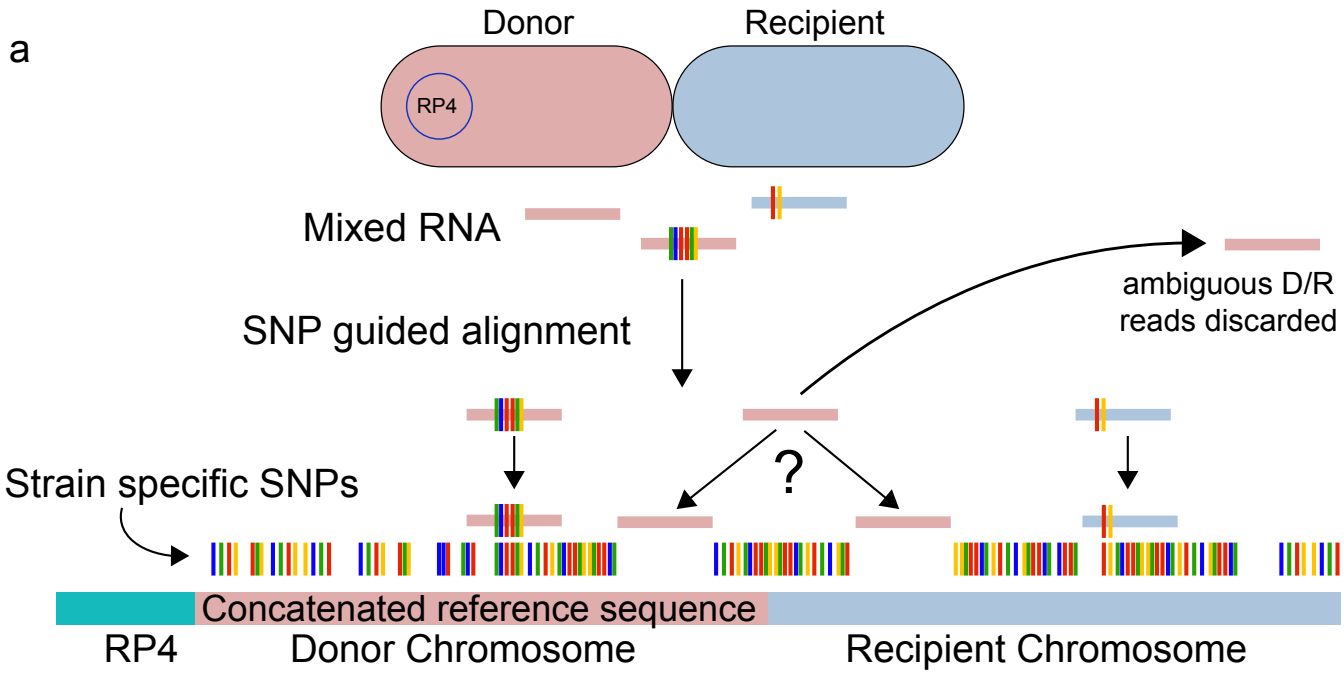
Donor
Recipient
RP4
Mixed RNA
SNP guided alignment
ambiguous D/R
reads discarded
?
Strain specific SNPs
Concatenated reference sequence
RP4
Donor Chromosome
Recipient Chromosome

b

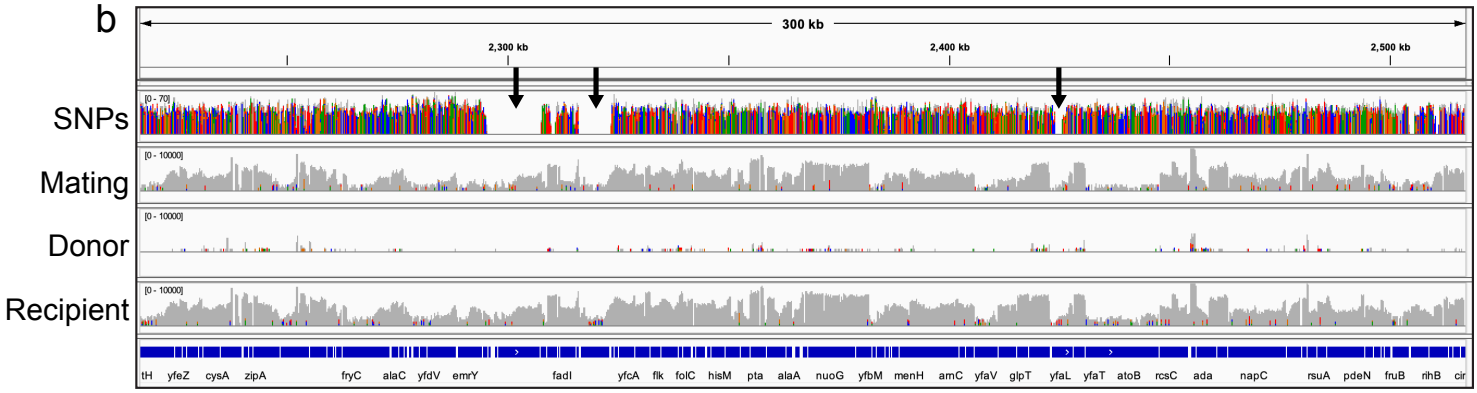
300 kb
2,300 kb
2,400 kb
2,500 kb
SNPs
Mating
Donor
Recipient
tH yfeZ cysA zipA fryC alaC yfdV emrY fadI yfcA flk folC hisM pta alaA nuoG yfbM menH amC yfaV glpT yfaL yfaT atoB rcsC ada napC rsuA pdeN fruB rihB cir

c

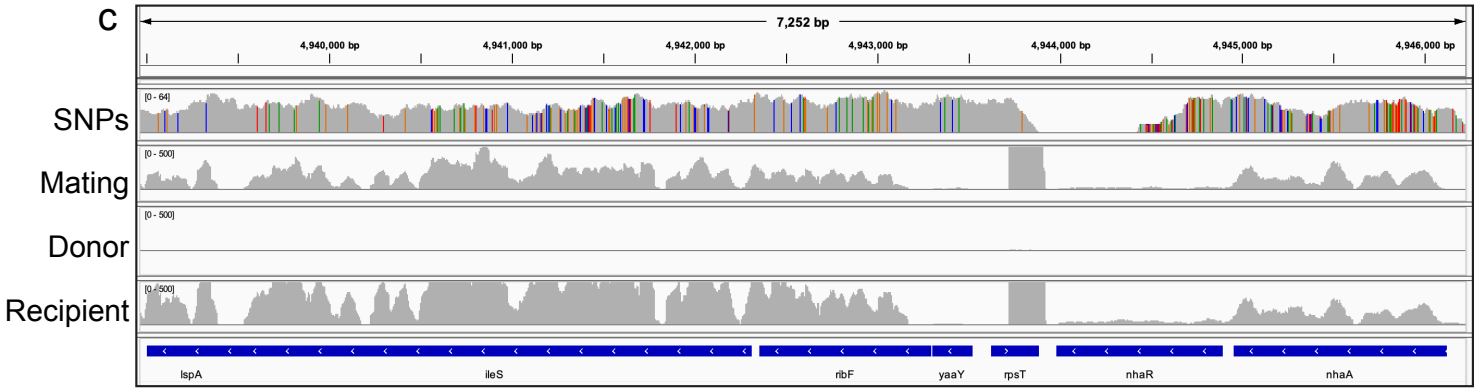
7,252 bp
4,940,000 bp
4,941,000 bp
4,942,000 bp
4,943,000 bp
4,944,000 bp
4,945,000 bp
4,946,000 bp
SNPs
Mating
Donor
Recipient
lspA ileS ribF yaaY rpsT nhaR nhaA

975

976 **Supplementary Figure 4: SNP and RNA-seq read alignment for HB101(pVS520) x DLL7555.**
977 a) schematic overview of RNA-seq alignment strategy. b-c) IGV plots depicting the coverage of
978 SNPs, and the alignment of mating, pure recipient and pure donor read coverage against a recipient
979 portion of the concatenated reference sequence at a global (b) and local (c) level. Gaps indicated
980 by black arrows in (b) represent genome segments entirely unique to DLL7555. The reads are log
981 scaled in (b).

982

983 **Table 1.** Bacterial strains and plasmids used in this work.

984

| Strain | Genotype/Characteristics | Reference |
|---|---|---|
| *E. coli* | | |
| DH5α | F- φ80*lac*ZΔM15Δ(*lac*ZYA-*arg*F)U169 *rec*A1 *end*A1 *hsd*R17($r_K$ ,$m_K^+$) *pho*A *sup*E44$\lambda^-$*thi*-1 *gyr*A96 *rel*A1 | Invitrogen |
| LT101 | $Rif^R$ derivative of HB101 | (61) |
| DLL7555 | ST73 $Rif^R$ clinical isolate of *E. coli* | (62) |
| *K. pneumoniae* | | |
| B5055 | Wild type *K. pneumoniae* O1:K2 | Provided by Richard Strugnell |
| B5055Δ*wzbc* | Non-encapsulated *wzbc* deletant mutant of B5055, $Km^R$ | Provided by Richard Strugnell, Adam Jenney, and Tania Uren |
| SGH10 | Hospital isolate of *K. pneumoniae* K1, ST23 | (63) |
| NUH26 | Hospital isolate of *K. pneumoniae* K5, ST1049 | (64) |
| NUH40 | Hospital isolate of *K. pneumoniae* K5, ST1049 | (29) |
| *A. baumannii* | | |
| AB5075 | Wild type *A. baumanii* KL25, $Ap^R$, $Erm^S$ | (65) |
| AB10132 | Capsular transposon mutant of AB5075, *wzC*::Tn*5*, $Tc^R$ | (66) |
| *Pasteurella multocida* | | |
| AL3145 | $Km^R$ derivative of VPI161 | (57) |
| AL2234 | VP161 capsular transposon mutant *hyaD*-Tn*7,* $Km^R$ | (57) |
| Plasmids | | |
| pWSK29 | $Ap^R$, low copy number cloning vector | (67) |
| pWSK29 P*traJ*GFPx3 | P*traJ*::*mGreenLantern*x3 | |
| pSU18 | $Cm^R$, medium copy number cloning vector | (68) |
| pSU18*mTagBFP2* | P*em7*::*mTagBFP2* | This work |

| | | |
|---|---|---|
| pVS520 | $Tc^R$, $Ap^S$, $Km^S$, derivative of RP4; $Tra^+$ $Mob^+$ | (61) |
| pMMB67EH | RSF1010 derived expression vector. $Ap^R$, $Mob^+$ | (69) |
| RFS1010-*erm* | $Erm^R$ derivative of RSF1010, $Mob^+$ | This work |
| pAL99S-*oriT* | $Spec^R$, $Mob^+$ derivative of pAL99S | This work |
| pMMB67EH*gfpmut3* | P*em7*::*gfpmut3* | This work |

985 **Note:** rif = rifampicin, km = kanamycin, tc = tetracycline, ap = ampicillin, cm = chloramphenicol,
986 erm = erythromycin, spec = spectinomycin
987
988
989